JHEP

Published for SISSA by Springer

Received: November 8, 2017
Revised: February 20, 2018
Accepted: March 1, 2018
Published: March 6, 2018

The case for future hadron colliders from $B \to K^{(*)}\mu^+\mu^-$ decays

B.C. Allanach,[a] **Ben Gripaios**[b] **and Tevong You**[a,b]

[a] *DAMTP, University of Cambridge, Wilberforce Road, Cambridge, CB3 0WA, U.K.*

[b] *Cavendish Laboratory, University of Cambridge, J.J. Thomson Avenue, Cambridge, CB3 0HE, U.K.*

E-mail: B.C.Allanach@damtp.cam.ac.uk, gripaios@hep.phy.cam.ac.uk, tty20@cam.ac.uk

Abstract: Recent measurements in $B \to K^{(*)}\mu^+\mu^-$ decays are somewhat discrepant with Standard Model predictions. They may be harbingers of new physics at an energy scale potentially accessible to direct discovery. We estimate the sensitivity of future hadron colliders to the possible new particles that may be responsible for the anomalies at tree-level: leptoquarks or Z's. We consider luminosity upgrades for a 14 TeV LHC, a 33 TeV LHC, and a 100 TeV pp collider such as the FCC-hh. In the most conservative and pessimistic models, for narrow particles with perturbative couplings, Z' masses up to 20 TeV and leptoquark masses up to 41 TeV may in principle explain the anomalies. Coverage of Z' models is excellent: a 33 TeV 1 ab^{-1} LHC is expected to cover most of the parameter space up to 8 TeV in mass, whereas the 100 TeV FCC-hh with 10 ab^{-1} will cover all of it. A smaller portion of the leptoquark parameter space is covered by future colliders: for example, in a $\mu^+\mu^- jj$ di-leptoquark search, a 100 TeV 10 ab^{-1} collider has a projected sensitivity up to leptoquark masses of 12 TeV (extendable to 21 TeV with a strong coupling for single leptoquark production).

Keywords: Beyond Standard Model, Heavy Quark Physics

ArXiv ePrint: 1710.06363

https://doi.org/10.1007/JHEP03(2018)021

JHEP03(2018)021

Contents

JHEP03(2018)021

1 Introduction

Perhaps the most convincing anomalies[1] observed in the LHC data thus far are those seen in ratios of branching ratios of semi-leptonic B-to-K or -K^* decays in LHCb [1, 2]. Though they involve sensitive measurements of rare processes, they are theoretically clean [3] and apparently a clear signal of violation of lepton universality, a principle that is sacrosanct in the gauge interactions of the Standard Model (SM). Moreover, the fact that such processes arise only at loop level in the SM means that, even though the observed deviations are large compared to the SM contribution, they could plausibly be explained by tree-level exchange of new particles at the TeV scale, with couplings of comparable size to those present in the SM.[2]

To put the measurement of these ratios in context, we summarise some of the related anomalies that preceded them: the first sign of a discrepancy appeared in the P_5' observable [11] of angular distributions in $B \to K^* \mu^+ \mu^-$ decays [12–16], designed in such a way that hadronic uncertainties cancel out and are under control. LHCb found a 3.4σ anomaly [14], supported somewhat at the 2σ level by a later BELLE measurement [17]. These were also consistent with a 3.2σ tension in $B_s \to \phi \mu^+ \mu^-$ [18]. Indeed, various global fits including LHCb, Belle, BaBar, CMS, and ATLAS data to a variety of $b \to s \mu^+ \mu^-$ kinematic observables indicated a non-zero value for a particular Wilson coefficient parameterising new physics coupling to left-handed quarks and muons, with a statistical pull $\gtrsim 4\sigma$ [19–28]. However, these observables could still have been heavily affected by residual theoretical uncertainties in the SM prediction. It was therefore notable that subsequent measurements

[1] Here, 'anomaly' refers to a measurement that is discrepant with respect to a Standard Model prediction.

[2] In contrast, apparent deviations seen in B-to-D decays [4–10] are comparable in size to SM tree-level contributions, and so seem to call for either an implausibly low scale of new physics or rather large couplings.

of the more theoretically clean ratios $R_K = BR(B \to K\mu^+\mu^-)/BR(B \to Ke^+e^-)$ and $R_{K^*} = BR(B \to K^*\mu^+\mu^-)/BR(B \to K^*e^+e^-)$ both observed deviations at around the 2.5σ level each [1, 2]. Moreover, fits to these two clean observables alone demonstrate a pull away from the SM at more than around 4σ on the *same* Wilson coefficient as the one from the global fit to the other observables [23–29]. This non-trivial consistency of the various anomalies goes some way towards explaining the level of interest in them, despite the significance of each individual measurement being low.

Even if the anomalies really are signatures of physics beyond the SM (and further data or a better understanding of the SM predictions may well indicate that they are not), we face the problem that the effects we see in B decays arise indirectly, via exchange of virtual states that are far from being on-mass-shell. To confirm the presence of new physics, and to begin the long, but tremendously exciting, programme of exploring Nature's next layer, we will need to produce the new particles directly on-shell, at a current or future collider. But in trying to plan for this, we must overcome a serious obstacle: the size of the effects being seen currently fixes neither the identity, nor the mass, nor the couplings of the new particles. So, at least without further consideration, not only do we not know what energy threshold a collider would need to reach to produce the new states, but also, even if we did know what energy were needed, we do not know what sort of detector, triggering, or cuts might be needed to make the discovery, nor which backgrounds we should strive to better control, nor how much luminosity might be required, and so on.

At least naïvely, we can make some progress on these issues by appealing to the arguments of perturbative unitarity: we know that the loop expansion of quantum field theory, and hence its predictability, breaks down when couplings approach values of 4π or so, and imposing this as an upper bound imposes an upper limit of $\mathcal{O}(100)$ TeV or so on the possible masses of new particles [24, 30]. A more refined analysis of partial wave unitarity shows that the scale of unitarity violation is actually ~ 80 TeV [30], and can be even lower in more specific model-dependent cases. Such unitarity arguments successfully predicted the appearance of a Higgs boson at the LHC [31, 32], but in the case of the physics inferred from $b-$decays, the cut-off scale is too high to form a similar no-lose theorem for the next generation of colliders.

Here, we attempt to carry out a rather more detailed analysis of the prospects for discovery of the new physics underlying the $b \to s\mu^+\mu^-$ anomalies, at current colliders or at proposed future facilities *while making as few assumptions about the models as possible*. Thus, in the most pessimistic possible scenario, we shall not assume universal couplings to different generations or minimal flavour violating couplings; we only include the minimal new physics that explains the $b \to s\mu^+\mu^-$ anomalies whilst refraining from adding more model-specific structure (that would typically only lower the scale of new physics or make it more easily discoverable unless decays are dominantly invisible). It turns out that (at least if one is prepared to accept a few simple assumptions along the way) one can make rather detailed and quantitative statements. This is possible for a variety of reasons, which we now describe in turn.

One reason is that, on the theory side, the possible underlying new physics models are rather limited, at least if one assumes that the new physics results in an effective low-

JHEP03(2018)021

energy operator coupling a left-handed quark current to a left-handed leptonic current. This assumption is reasonable not only because doing so results in a very good fit to the data (in fact, the best fit to the data, as discussed above), but also because it is highly plausible theoretically, given that the basic objects in the SM are the distinct left- and right-handed fermion multiplets. With this operator, one is limited at tree-level to models with either vector leptoquarks (LQs), scalar LQs or models with new neutral vector particles (Z's) coupling to left-handed currents.

Within this limited range of possible models, there is still a great deal of room to manoeuvre in terms of choosing couplings. But again we can make headway by adopting a conservative approach, leading to predictions that are as pessimistic as possible for these minimal models. For LQ models, for example, it is perfectly consistent mathematically (although highly unlikely in practice), that the LQ has only the Yukawa couplings needed to explain the anomalies, namely to the left-handed lepton doublet containing the muon mass eigenstate[3] and to the two left-handed quark doublets containing the b- and s- quark mass eigenstates. The presence of any other Yukawa couplings (especially those to electrons or light quarks) is likely only to increase the discoverability of the LQ, by providing additional channels for production at a hadron colliders and additional final states that are relatively easy to observe.[4] For Z' models, things are a little more complicated, because it is not possible to switch on a coupling to b and s quarks alone: any assignment of charges under the corresponding $\mathrm{U}(1)'$ gauge symmetry to the three quark doublets in the electroweak basis will lead to other couplings being present in the mass basis.[5] So we consider two different conservative models featuring Z' states. In the first model, we allow only a bs coupling in the mass basis. Though mathematically inconsistent, strictly speaking, no inconsistencies arise in the collider phenomenology that we consider here. In the second model, we assume that there is only a coupling to a single generation of quark and lepton doublets (which are those that are mostly b and μ, respectively) and assume that all of the CKM rotation takes place in the down quark sector. Again, for both models our expectation is that any couplings that are additionally present are likely to increase discoverability.[6]

There are also reasons on the experimental side for why a more detailed analysis of the prospects for discovery at a current or future collider is possible. Most importantly, we can extrapolate based on the performance of current colliders, making the conservative assumption that the detector performance will remain roughly the same. This extrapolation is simplified by the fact that the discovery potential of a given machine is largely fixed by our understanding of the backgrounds. In the particular case of searching for a narrow

[3]The anomalies in the ratios R_K and R_{K^*} could, *a priori* be due to physics in either muonic or electronic operators. But the presence of additional anomalies in purely muonic processes [12–14, 18], together with the difficulty of accommodating large deviations in flavour physics processes involving electrons, both lead us to assume that the new physics states couple to muons rather than electrons.

[4]There is a danger, e.g. by adding charm/tau couplings, of diluting the LQ decays to clean final states, but to study this fully would require an analysis at a level of detail that seems overly premature.

[5]Consistency of the theory also requires additional particles for the $\mathrm{U}(1)'$ gauge symmetry to be anomaly-free [33].

[6]A Z' may always decay into a hidden sector, and although LQ decays must include coloured final states these could nevertheless be soft enough to still evade detection.

JHEP03(2018)021

resonance in a given channel at a given centre of mass energy, for example, what is needed is an understanding of the different background contributions (and their uncertainties) in that channel at that centre-of-mass (CM) energy. These backgrounds come, of course, from a combination of the underlying SM physics, which we understand well, together with its manifestation in the detector, which we assume remains similar to current detector performance at the extrapolated energies. This extrapolation is further helped by the fact that the SM is essentially scaleless at the multi-TeV energies that we consider, so that extrapolation amounts to a simple re-scaling, using a procedure outlined and validated in ref. [34]: in a nutshell, the idea is that the equivalent CM energy at a future collider that gives the same number of background events as a given CM energy in a current search will also yield the same upper limit on a putative signal cross section at that equivalent CM energy (this is similar to a method previously suggested [35]).

Proceeding in this way, we are able to obtain a number of simple results, that we believe to be robust within our reasonable assumptions. We find that a 33 TeV high energy upgrade to the LHC[7] should be able to cover most of the Z' parameter space that is under perturbative control in our first model with only bs couplings, while it can cover all of the parameter space for our second model with CKM-induced couplings to the first two generations of down-type quarks. A 100 TeV hadron collider has complete coverage for both models; it can therefore discover or exclude any perturbative Z' explanation of the anomalies (where the Z' width does not exceed 10% of its mass). On the LQ side, considering only pair production via QCD interactions, we find that masses up to 12 TeV can be ruled out in the scalar case. Limits from single production are more model-dependent but become important for $\mathcal{O}(1)$ couplings, with sensitivity to LQ masses up to 21 TeV for coupling values up to 4π.

All of this assumes, of course, that the anomalies currently observed are really due to new physics. If it turns out that they are not, the exercise that we have carried out becomes much more academic. But even so, we think that it gives a useful illustration of the complementarity between indirect and direct searches and how one can use anomalies that may plausibly arise in the future, wherever they might occur, to build a concrete strategy for future colliders and particle physics in general.[8]

The paper is organised as follows: in section 2 we summarise the effective field theory description of the possible new physics parameterising the anomalies, justifying our choice of operator, then describing the possible models that may explain the discrepancy with the SM. In section 3 we describe the extrapolation method that we adopt for our study, and present our results. We conclude with a summary and outlook in section 4.

[7]Studies to date have assumed a 33 TeV centre of mass energy, which we choose as a benchmark, but in the future we shall also consider the reduced energy of 27 TeV that can be attained using the 16 T beam magnets currently being designed for FCC-hh.

[8]For some reviews of physics at a 100 TeV hadron collider, see for example refs. [36–40]. The indirect sensitivity of future lepton colliders has been explored in e.g. refs. [41–46].

JHEP03(2018)021

2 New physics in B anomalies

2.1 Effective field theory description

Processes involving $b \to s l^+ l^-$ transitions can be described by a low-energy effective Lagrangian below the weak scale with the $W^\pm$ boson, Z boson, Higgs boson and top quark integrated out.[9] The relevant indirect effects of new physics (and SM weak interactions) are encapsulated by the following four-fermion operators,[10]

$$\begin{aligned}\mathcal{L}_{\text{eff}} \supset & \sum_{l=e,\mu,\tau} \sum_{i=L,R} \sum_{j=L,R} \frac{c^l_{ij}}{\Lambda^2_{l,ij}} \mathcal{O}^l_{ij} \,, \\ & = V_{tb} V^*_{ts} \frac{\alpha_{\text{EM}}}{4\pi v^2} \sum_{l=e,\mu,\tau} \left(\bar{c}^l_{LL} \mathcal{O}^l_{LL} + \bar{c}^l_{LR} \mathcal{O}^l_{LR} + \bar{c}^l_{RL} \mathcal{O}^l_{RL} + \bar{c}^l_{RR} \mathcal{O}^l_{RR} \right) \,, \end{aligned} \tag{2.1}$$

where

$$\mathcal{O}^l_{ij} = (\bar{s} \gamma^\mu P_i b)(\bar{l} \gamma_\mu P_j l) \,. \tag{2.2}$$

In the second line we defined dimensionless Wilson coefficients $\bar{c}^l_{ij}$ normalised by a conventional factor involving elements of the CKM matrix V and ratio of the EFT cut-off scale Λ to the weak scale $v \simeq 174\,\text{GeV}$ such that

$$\bar{c}^l_{ij} = \frac{4\pi}{\alpha_{\text{EM}} V_{tb} V^*_{ts}} \frac{v^2}{\Lambda^2} c^l_{ij} \simeq \frac{(36\ \text{TeV})^2}{\Lambda^2} c^l_{ij} \,. \tag{2.3}$$

If new particles with couplings to leptons and quarks of size g_{NP} are integrated out at tree-level, then $c^l_{ij} \sim \mathcal{O}(g^2_{\text{NP}})$ and since, according to our criterion, the limit of validity of perturbative unitarity is reached when $g_{\text{NP}} \sim 4\pi$, this sets an approximate upper limit on the cut-off scale[11] of

$$\Lambda_{\text{max}} \sim \frac{450\ \text{TeV}}{\sqrt{\bar{c}^l_{ij}}} \,. \tag{2.4}$$

For example, with $|\bar{c}^l_{ij}| \simeq 1.33$, as found in certain best fit values [28], we have $\Lambda_{\text{max}} \lesssim 390\,\text{TeV}$. A more detailed analysis of partial wave unitarity yields a 80 TeV bound [30]. However, other experimental and theoretical bounds will lead to a more restrictive upper limit on the scale of new physics, as we discuss below.

Many global fits to the flavour anomalies have been performed e.g. [19–28]. Ref. [28], for example, finds that an individual fit to one operator at a time in the muonic sector favours $\bar{c}^\mu_{LL} \simeq -1.33$ at $> 4\sigma$ significance. A similar conclusion holds for a global fit allowing several operators to vary simultaneously, which then allows an additional sub-dominant contribution from $\bar{c}^\mu_{LR}$ (though $\bar{c}^\mu_{LR}$ alone cannot explain the anomalies since it predicts an

[9] If the new physics responsible for the B anomalies is not at low energies [47–51] then the low-energy effective theory can be matched to the SM effective field theory (EFT) [29, 52, 53].

[10] The relation to coefficients of the $\mathcal{O}_{9,10}$ operators in another commonly used basis is given by $c_{9,10} = \pm(c_{LL} \pm c_{LR})/2$ [28].

[11] The perturbativity condition is sometimes also taken to be $g^2_{\text{NP}} \sim 4\pi$ [24], in which case the cut-off is $\Lambda_{\text{max}} \sim 127\ \text{TeV}/\sqrt{\bar{c}^l_{ij}} \sim 110\ \text{TeV}$.

JHEP03(2018)021

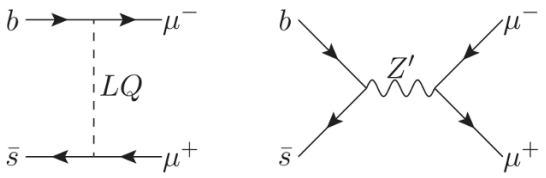

Figure 1. Feynman diagrams of the two tree-level possibilities for mediating an effective operator that explains discrepancies in $B \to K^{(*)}\mu^+\mu^-$ decays as compared to SM predictions. The diagram on the left hand side shows mediation by a scalar LQ, whereas the right-hand side shows mediation by a flavour dependent Z'.

enhancement in both R_K and R_{K^*}). The coefficients $\bar{c}^{\mu}_{RR}$ and $\bar{c}^{\mu}_{RL}$ are disfavoured by the relative directions of their pulls on R_K and R_{K^*}.

In individual fits to $R_{K^{(*)}}$ for electronic operators, the anomalies are also well described by either $\bar{c}^{e}_{LL}, \bar{c}^{e}_{LR}$, or $\bar{c}^{e}_{RR}$ (though the latter two require larger coefficient values due to their suppressed SM interference). Nevertheless the significance decreases substantially in a global fit including other observables, which shows a clear preference for non SM contributions in decays to muons rather than in decays to electrons.[12] We shall therefore assume new physics to reside solely in the muonic sector and in $\bar{c}^{\mu}_{LL}$ in particular. This restricts the type of heavy particles that can be integrated out to give $\bar{c}^{\mu}_{LL}$ in the EFT, as we discuss next.

2.2 Z' and LQ models to explain the discrepancy

At tree level there are only a few candidates to consider for mediating the interactions responsible for the B anomalies. These are so-called LQs, that can be either scalar or vector, and Z' vector bosons. We shall assume that in each scenario, the new fields are *unique* representations of the Lorentz group and the SM, i.e. we are not considering multiple identical fields. Feynman diagrams for the relevant interactions are shown in figure 1. When the mass of the LQ or Z' is much larger than the mass of the decaying B meson, matching to the effective field theory in eq. (2.1) should provide an accurate approximation to order m_B/Λ, where Λ is the mass of the LQ or Z'.

Other explanations for the anomalies arise at the loop level. In this case, in order to explain the required size of the non-standard contributions to $B \to K^{(*)}\mu^+\mu^-$ decays, the new particles mediating the interaction must be relatively light and so are more easily discoverable; we therefore restrict our attention to the more conservative case of heavier tree-level induced new physics.

The preference of fits for the $\mathcal{O}^{\mu}_{LL}$ operator picks out particular combinations of quantum numbers allowed for the LQs [23, 25, 28] . For the scalar case this is the triplet LQ S_3, with quantum numbers $(\bar{3}, 3, \frac{1}{3})$ under $\mathrm{SU}(3)_c \times \mathrm{SU}(2)_L \times \mathrm{U}(1)_Y$, whose Yukawa couplings to the quark and lepton doublets Q and L are of the form

$$y_3 QLS_3 + y_q QQS_3^{\dagger} + \text{h.c.}\,. \tag{2.5}$$

[12] Ref. [54] first pointed out an indication of lepton flavour universality violation from a global fit, though more data is needed to conclusively establish this [55].

JHEP03(2018)021

The term proportional to y_q induces proton decay and is typically set to zero by imposing baryon number conservation. For the vector case, the $\mathcal{O}_{LL}$ operator may be generated by integrating out a singlet V_1 or a triplet V_3 with quantum numbers $(\bar{3}, 1, \frac{2}{3})$ and $(3, 3, \frac{2}{3})$, respectively. The possible couplings are

$$y_3' V_3^\mu \bar{Q}\gamma_\mu L + y_1 V_1^\mu \bar{Q}\gamma_\mu L + y_1' V_1^\mu \bar{d}\gamma_\mu l + \text{h.c.}\,, \tag{2.6}$$

where d and l are the right-handed down quark and right-handed charged lepton, respectively. We focus on the couplings generating our operator of interest, $\mathcal{O}_{LL}^\mu$. Integrating out the LQs with mass M and coupling y gives the Wilson coefficient [25]

$$\bar{c}_{LL}^\mu = \kappa \frac{4\pi v^2}{\alpha_{\text{EM}} V_{tb} V_{ts}^*} \frac{|y|^2}{M^2}\,, \tag{2.7}$$

where $\kappa = 1, -1, -1$ and $y = y_3, y_1, y_3'$ for S_3, V_1, V_3, respectively.

For Z' vector bosons, the minimal Lagrangian containing the couplings responsible for generating $\mathcal{O}_{LL}^\mu$ at low energy is given by [28, 56].

$$\mathcal{L}_{Z'}^{\text{min.}} \supset \left(g_L^{sb} Z'_\rho \bar{s}\gamma^\rho P_L b + \text{h.c.} \right) + g_L^{\mu\mu} Z'_\rho \bar{\mu}\gamma^\rho P_L \mu\,, \tag{2.8}$$

which contributes to the $\mathcal{O}_{LL}^\mu$ coefficient with

$$\bar{c}_{LL}^\mu = -\frac{4\pi v^2}{\alpha_{\text{EM}} V_{tb} V_{ts}^*} \frac{g_L^{sb} g_L^{\mu\mu}}{M_{Z'}^2}\,. \tag{2.9}$$

Simplified limits upon Z' explanations of the R_K anomalies were considered in ref. [57].

Couplings to some other SM fermions are required by $\text{SU}(2)_L$ invariance and some additional couplings to other flavours of quark are necessarily generated by CKM rotations when going from the weak to the mass eigenbasis. However, given that these additional interactions are more model-dependent than the ones we write above, we shall take the Lagrangian of eq. (2.8) as our minimal model (which we call the naïve Z' model). Although strictly, the model is incomplete without the additional couplings, the naïve Z' model is a conservative case to study; additional couplings to SM states will only raise the Z' production cross-section, by including couplings to the first two quark generations, and increase the total decay width which is in tension with other constraints (in particular, the perturbativity constraint and no Landau poles below the Planck scale). An exception to this is if the Z' dominantly decays into invisible particles such as dark matter [56]. In that case, the detectable cross-section times branching ratio for the $\mu^+\mu^-$ final state will be reduced. However, modulo this proviso, if a future collider covers some portion of the viable parameter space of the naïve Z' model, then we know that a more realistic and complete model will also be covered there.

To illustrate the size of such effects in a more complete model we shall also consider the case where the Z' couples only to third generation left-handed quarks and left-handed muons and neutrinos in the weak basis. The couplings to the first two generations of quarks then arise from CKM rotations, which we assume to be entirely in the down sector. Additionally, if we assume that in the weak eigenbasis all left-handed lepton mixing resides

JHEP03(2018)021

in the neutrino sector, we have a logically consistent model which contains only a coupling to left-handed muons and some family mixture of neutrinos. The precise family mixture of neutrinos is immaterial for collider experiments, since each neutrino is essentially massless and leaves an identical missing momentum signature in detectors. The relevant interaction terms in the Lagrangian for this '$33\mu\mu$' model are given by

$$\begin{aligned}\mathcal{L}_{Z'}^{33\mu\mu} \supset g_L^q Z'_\rho \Big[& \bar{t}\gamma^\rho P_L t + |V_{tb}|^2 \bar{b}\gamma^\rho P_L b + |V_{td}|^2 \bar{d}\gamma^\rho P_L d + |V_{ts}|^2 \bar{s}\gamma^\rho P_L s \\ & + \left(V_{tb}V_{ts}^* \bar{b}\gamma^\rho P_L s + V_{ts}^* V_{td} \bar{d}\gamma^\rho P_L s + V_{tb}V_{td}^* \bar{b}\gamma^\rho P_L d + \text{h.c.}\right) \\ & + g_L^{\mu\mu} \left(\bar{\mu}\gamma^\rho P_L \mu + \sum_{i,j} \bar{\nu}_i U_{i\mu} \gamma^\rho P_L U_{\mu j}^* \nu_j \right) \Big], \end{aligned} \tag{2.10}$$

where U denotes the PMNS matrix involved in lepton mixing.

With these LQ and Z' models in hand, we now turn to their discovery prospects. Some previous studies have examined the 13 TeV LHC's ability to discover other effects caused by new physics involved in the errant $b-$decays assuming any mediator is not too heavy. In ref. [56], LHC bounds on Z' models that explain the $b-$anomalies from di-muon resonances were placed, assuming a universal Z' coupling to the first two generations of quarks. Ref. [58] also examined current LHC constraints on LQs and performed naïve re-scaling to estimate the sensitivity at higher luminosities in models which explain both the $b \to s\mu^+\mu^-$ anomalies that we consider and additional ones inferred in $b \to c\tau\bar{\nu}_\tau$ decays.[13] Ref. [59] also examined the LHC's ability to detect scalar LQs of 1 TeV mass of the type that we shall examine. Ref. [60] examines the di-lepton final state for effective field theory operators caused by LQs or Z's. Some sensitivity is found under the assumption of minimal flavour violation for light enough Z's.

In our study we look towards future colliders at higher luminosity and energy. In the next section we shall estimate the projected limits on the Z' and LQ masses in our conservative models by extrapolating from direct searches at the LHC.

3 Projected sensitivity on Z' and LQs

3.1 Limit extrapolation method

We follow the approach of ref. [34] to extrapolate the limits on direct searches for new resonances at the LHC to higher energy and luminosity. The method assumes that such a limit is entirely driven by the number of background events, so that finding the equivalent mass at a future collider that gives the same background as a given mass in a current search will also yield the same upper limit on a putative signal cross section at that equivalent mass.

[13] In the present paper, we do not consider physics due to these charged current decays because the size of those effects requires a low mass scale that would make the new physics responsible more easily discoverable than the source of the neutral current b-anomalies.

JHEP03(2018)021

Concretely, the background cross-section at a resonance mass M and centre of mass collision energy $\sqrt{s}$ is

$$\sigma_B(M,s) \propto \sum_{i,j} \int_{M^2-\Delta\hat{s}}^{M^2+\Delta\hat{s}} d\hat{s} \frac{dL_{ij}}{d\hat{s}} \hat{\sigma}_{ij}(\hat{s}) \,, \tag{3.1}$$

where $\hat{\sigma}_{ij}(\hat{s})$ is the partonic cross section for background processes, produced by partons i and j evaluated at a partonic centre of mass energy $\sqrt{\hat{s}}$ and the parton luminosity function $dL_{ij}/d\hat{s}$ for the initial state parton pair labelled by i and j is given by

$$\frac{dL_{ij}}{d\hat{s}} = \frac{1}{s} \int_{\hat{s}/s}^{1} \frac{dx}{x} f_i\left(x,\mu^2\right) f_j\left(\frac{\hat{s}}{sx},\mu^2\right). \tag{3.2}$$

We set the factorisation scale $\mu = \sqrt{\hat{s}}$. We assume that the resonance is sufficiently narrow, $\Delta\hat{s} \ll M^2$, such that the partonic luminosity is approximately constant in the integration region. Since the background consists of SM processes at energies far above the weak scale, the partonic cross-section should scale like $\hat{\sigma}_{ij} \propto 1/\hat{s}$. The total background cross-section then simplifies to

$$\sigma_B(M,s) \propto \frac{\Delta\hat{s}}{M^2} \sum_{i,j} C_{ij} \frac{dL_{ij}}{d\hat{s}}(M,s) \,, \tag{3.3}$$

where $C_{ij} = \hat{s}\hat{\sigma}_{ij}$ is approximately constant. The number of background events at a given luminosity L is $N_B = L \cdot \sigma_B(M,s)$. If a 95% confidence level (CL) limit on a signal cross-section is set for a given resonance mass M_0 at a present collider (with energy $\sqrt{s_0}$ and luminosity L_0), then we find the equivalent mass M' for which the limit applies at a future collider (with energy $\sqrt{s'}$ and luminosity L') by the assumption that the same limit is applicable when $N'_B = N^0_B$, i.e.

$$L_0 \cdot \sum_{i,j} C_{ij} \frac{dL_{ij}}{d\hat{s}}(M_0,s_0) = L' \cdot \sum_{i,j} C_{ij} \frac{dL_{ij}}{d\hat{s}}(M',s') \,. \tag{3.4}$$

The fixed relative width $\Delta\hat{s}/M^2$ and other prefactors have cancelled out, leaving a straightforward equation to solve for M'. The constants C_{ij} can be normalised such that they represent the relative weights of the contributions from each parton pair. In practice, the C_{ij} are obtained using `MadGraph` to obtain the fraction of each background contribution to the total partonic cross-section.[14]

This method introduces some arbitrariness in the starting point of the extrapolated exclusion curve, since it depends on a re-scaling by the luminosity ratio L_0/L'. If $L' = L_0$ then the smallest mass $M_{0\min}$ at the lower end of the current collider sensitivity will be extrapolated to the starting point $M'_{\min}$ of the exclusion curve at the future collider. On the other hand if $L' > L_0$ then the starting point will be at a higher mass point, while $L' < L_0$ would reach lower masses. A conservative procedure to account for this artificial effect is to smoothly vary the future collider luminosity up to L' during the extrapolation

[14]Tables of C_{ij} values for the channels considered below can be found in files attached to the arxiv submission or upon request to the authors.

JHEP03(2018)021

and take the strongest limit for each mass point, which only affects the limit for masses below M'_{min}, and in any case is more conservative than a realistic limit [34].

This extrapolation method has many approximations: one of the largest being that changes of efficiencies and acceptances with centre of mass energy are neglected. It has been validated against a cut-and-count-based analysis for di-lepton searches in ref. [34], where agreement is found up to a factor of two for a width of $\Delta\hat{s}/M^2 = 10\%$. Results from the approximate method outlined here can then be trusted in so far as a more complete analysis does not give limits too far off from a cut-and-count-based one. While more realistic experimental analyses will certainly use more refined methods that go beyond our assumptions, the approximation is sufficient for a rough estimate of future collider sensitivity and should help motivate a more detailed study.

3.2 Z' sensitivity

We extrapolate limits from the ATLAS 13 TeV search in the di-muon final state at $\sqrt{s} =$ 13 TeV and 3.2 fb^{-1} [61].[15] The dominant backgrounds come from Drell-Yan, $t\bar{t}$ and di-boson production. Using the procedure described in section 3.1, we obtain the projected limits displayed in figure 2. The solid black line in the left plot is the current 95% CL limit from the ATLAS 13 TeV analysis. In dashed black is the projected limit for HL-LHC at 14 TeV with 3 ab^{-1}, while the solid and dashed lines in cyan are for the HE-LHC at 33 TeV with 1 and 10 ab^{-1}, respectively. The plot on the right shows the corresponding FCC-hh 100 TeV limits in solid (dashed) red for 1 (10) ab^{-1}. The shaded regions on the curves indicate the point at which the extrapolation method underestimates the actual limit at low masses, as explained in section 3.1.

One may note various features in figure 2 that might seem surprising *prima facie*: for example, it appears that the 14 TeV 3 ab^{-1} HL-LHC can reach lower in $\sigma \times BR$ than the 10 ab^{-1} 33 TeV HE-LHC for $M < 6$ TeV. This is caused by the behaviour of regions dominated by high backgrounds at lower masses: if one increases the centre of mass energy from the LHC to higher collider energies then this background-dominated region will correspondingly move to higher masses. On the other end we see that at the highest values of M the HE-LHC is the most sensitive, as expected. While these sensitivity limits are purely a function of the background, the actual limit set for a given Z' mass and coupling also depends on the signal cross-section, which is larger at higher collider energies. Therefore a lower-energy collider whose limit curve reaches further down than that of a higher-energy collider does not necessarily translate to better sensitivity in a model's parameter space.

The actual Z' mass that can be excluded for a B-anomaly-compatible model depends on the specific couplings of the Z' and its total decay width. We calculated the Drell-Yan cross-section for $pp \to Z' \to \mu^+\mu^-$ as a function of these couplings using the following expression in the narrow width approximation, cross-checked with `MadGraph` [62],

$$\sigma_{pp\to Z'\to\mu^+\mu^-} = 16\pi^2 \sum_{i,j} \left(\frac{S_{Z'}}{S_i S_j} \frac{C_{Z'}}{C_i C_j} \frac{\Gamma_{Z'\to\bar{q}_i q_j}}{M_{Z'}} \frac{1}{s} \frac{dL_{ij}}{d\tau}\bigg|_{\tau=M^2_{Z'}/s} \right) \text{BR}(Z' \to \mu^+\mu^-)\,, \quad (3.5)$$

[15] We used the obtained LHC limit rather than the expected sensitivity. However, since the limit and the sensitivity are close (within about 2σ), this is a reasonable approximation.

JHEP03(2018)021

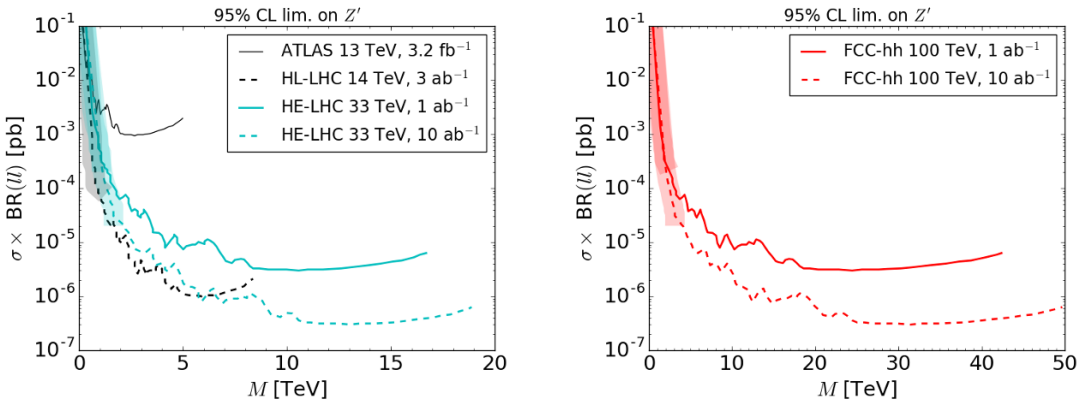

Figure 2. Projected sensitivity of di-muon resonance searches of some future hadron colliders to Z' models that may explain anomalous $B \to K^{(*)}\mu^+\mu^-$ decay results for the luminosities and centre of mass energies given in the legend. Shaded parts of the curve indicate the conservative extrapolation method at low masses that underestimates the actual limit.

where S_i and C_i are the number of spin and colour degrees of freedom of parton i respectively, and the parton luminosity function is

$$\frac{dL_{ij}}{d\tau} = \int_\tau^1 \frac{dx}{x} f_i\left(x, \mu^2\right) f_j\left(\frac{\tau}{x}, \mu^2\right) . \tag{3.6}$$

The decay rate for Z' into fermions with coupling g_f, assuming $m_f \ll M_{Z'}$, is given by

$$\Gamma_{Z' \to \bar{f}_i f_j} = \frac{C}{24\pi} g_f^2 M_{Z'} , \tag{3.7}$$

where the colour factor C is 3 for quarks and 1 for leptons. For the parton distribution functions $f(x, \mu^2)$ we use the 5-flavour NNPDF2.3LO ($\alpha_s(M_Z) = 0.119$) set [63] with `LHAPDF` [64] and fix the factorisation scale to be $M_{Z'}^2$. We consider b quarks to be in the initial PDFs of the proton, thus re-summing large logarithms on the initial b quark line [65]. The Feynman diagram for hadron collider production is therefore identical to the right-hand plot of figure 1.

Using these expressions and the extrapolated limits of figure 2, the resulting parameter space for the naïve model is shown in figure 3. As discussed in section 2.2, we take the naïve model of eq. (2.8) defined by only a Z' coupling to $\bar{b}s + \bar{s}b$ and $\mu^+\mu^-$, and nothing else, as the most conservative possible case. While other couplings should necessarily be present, the naïve Z' serves as a useful scenario to assess the sensitivity of a future collider since any model that seeks to explain the B-anomalies must have at least these couplings, while other interactions are more model-dependent.

The line and colour coding for figure 3 is as follows: the blue-shaded region covering the area vertically towards the right corresponds to the extrapolated 95% CL limit for the highest luminosity at the collider energy shown in the plot title; the grey-shaded region excluding the area horizontally towards the top is where the Z' width exceeds 10%; the vertical red region is excluded by too large a contribution to $B_s - \bar{B}_s$ mixing which constrains $|\bar{g}_L^{sb}| \lesssim \sqrt{2} M_{Z'}/(210 \text{ TeV})$ [28]; the green region is compatible with the B anomaly within

JHEP03(2018)021

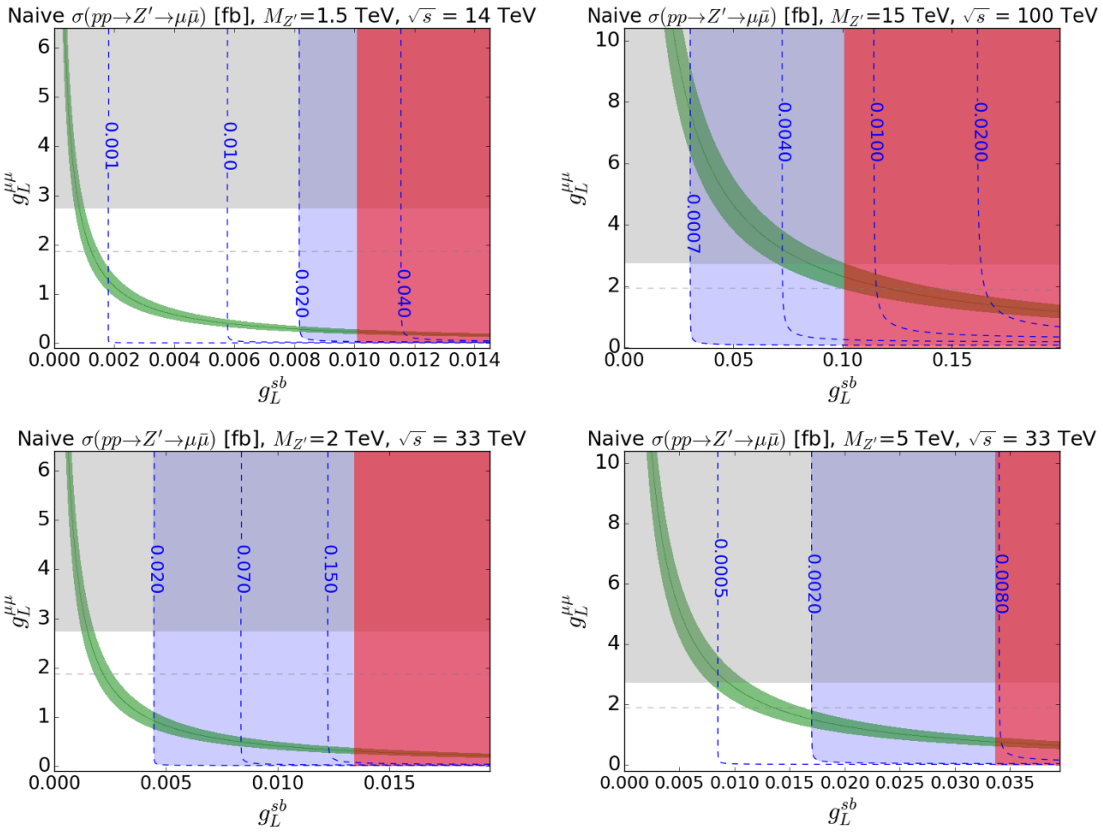

Figure 3. Parameter space of Z' models that explain $B \to K^{(*)}\mu^+\mu^-$ decay results for the naïve Z' model for different future colliders and $M_{Z'}$ assumptions. The horizontal (grey) shaded region violates the narrow width approximation. The vertical (red) region extending to the right hand side of each plot shows the limit coming from $B_s - \bar{B}_s$ mixing measurements. The (green) curve displays the region that fits $B \to K^{(*)}\mu^+\mu^-$ decay results. Above the dashed (grey) horizontal line, the coupling reaches a Landau pole below the Planck scale. The darker dashed (blue) contours are labelled with the expected production cross-section times branching ratio in fb. The shaded (blue) region shows the expected sensitivity at the future collider from di-muon resonance searches derived from figure 2.

1σ of the best fit value of ref. [28]; the blue (mostly) vertical dashed lines are the contours of cross-section in units of femtobarns; and the horizontal grey dashed line is where [56]

$$\frac{\Gamma_{Z'}}{M_{Z'}} \lesssim \frac{\pi}{2}\frac{1}{\ln(M_{pl}/M_{Z'})}\,, \tag{3.8}$$

indicating that the Z' couplings will hit a Landau pole before the Planck scale; the region above this dashed line is therefore theoretically disfavoured. This last condition is model dependent as the Feynman diagram contributing to the decay width, given by the imaginary part of the Z' propagator, will also contribute to the renormalisation group running from the real part of the propagator. While this perturbativity condition is weakened by new vector bosons contributing to the running, it is strengthened by the addition of scalars or fermions.

JHEP03(2018)021

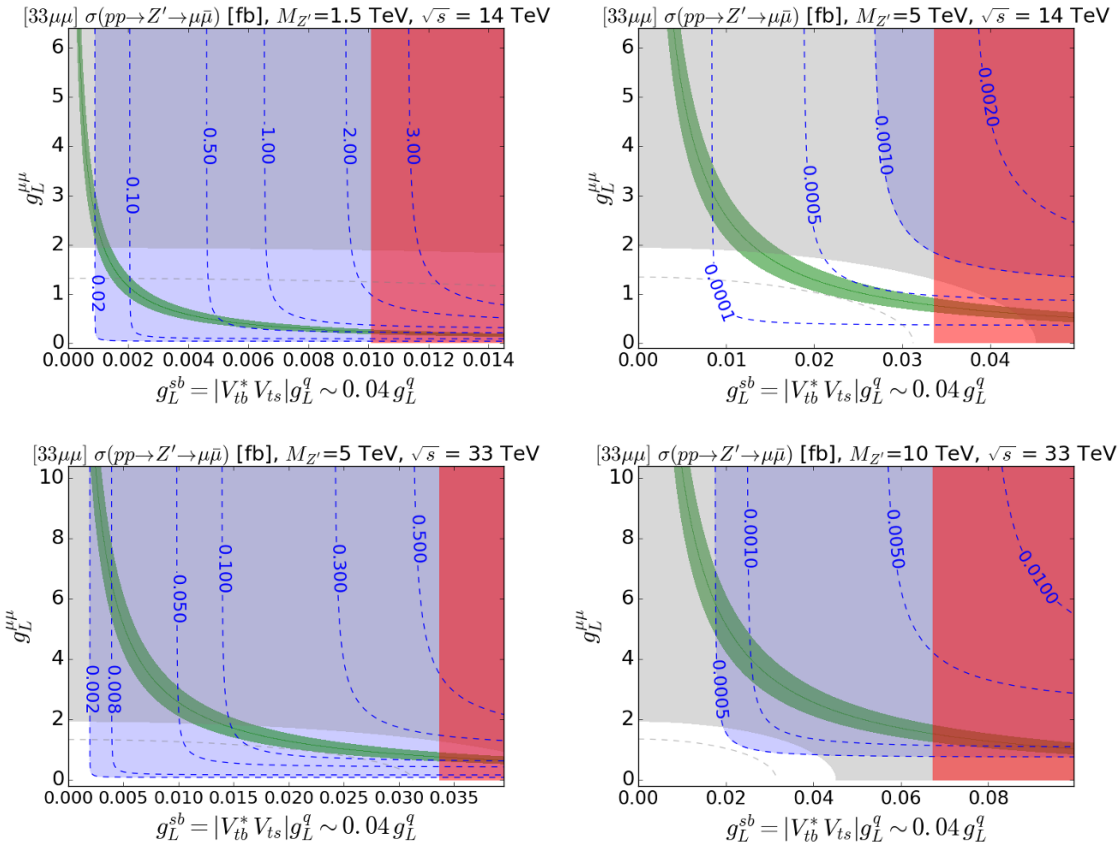

Figure 4. Parameter space of Z' models that explain $B \to K^{(*)}\mu^+\mu^-$ decay results for the $33\mu\mu$ model for different future colliders and $M_{Z'}$ assumptions. The horizontal (grey) shaded region violates the narrow width approximation. The vertical (red) region extending to the right hand side of each plot shows the limit coming from $B_s - \bar{B}_s$ mixing measurements. The (green) curve displays the region that fits $B \to K^{(*)}\mu^+\mu^-$ decay results. Above the dashed (grey) horizontal line, the coupling reaches a Landau pole below the Planck scale. The darker dashed (blue) contours are labelled with the expected production cross-section times branching ratio in fb. The shaded (blue) region shows the expected sensitivity at the future collider from di-muon resonance searches derived from figure 2.

The top left plot in figure 3 indicates that the HL-LHC at 14 TeV and 3 ab^{-1} is barely sensitive to a naïve Z' when its mass is 1.5 TeV. This may seem low but we recall that in the naïve model the only production mechanism for Z' in Drell-Yan is through b and s initial state partons.[16] On the other extreme end of collider reach is the FCC-hh at 100 TeV, shown on the top right for $M_{Z'} = 15$ TeV. We see that a 15 TeV Z' is at the limit of being anomaly-compatible and evading the constraints from both $B_s - \bar{B}_s$ mixing and Landau poles. Nevertheless, the blue region corresponding to FCC-hh with 10 ab^{-1} can easily cover all of the parameter space of interest. For lower luminosities the sensitivity can be read off from the cross-section contours and the corresponding limits in figure 2.

[16]For a study of other possible production mechanisms with these couplings, see ref. [66].

JHEP03(2018)021

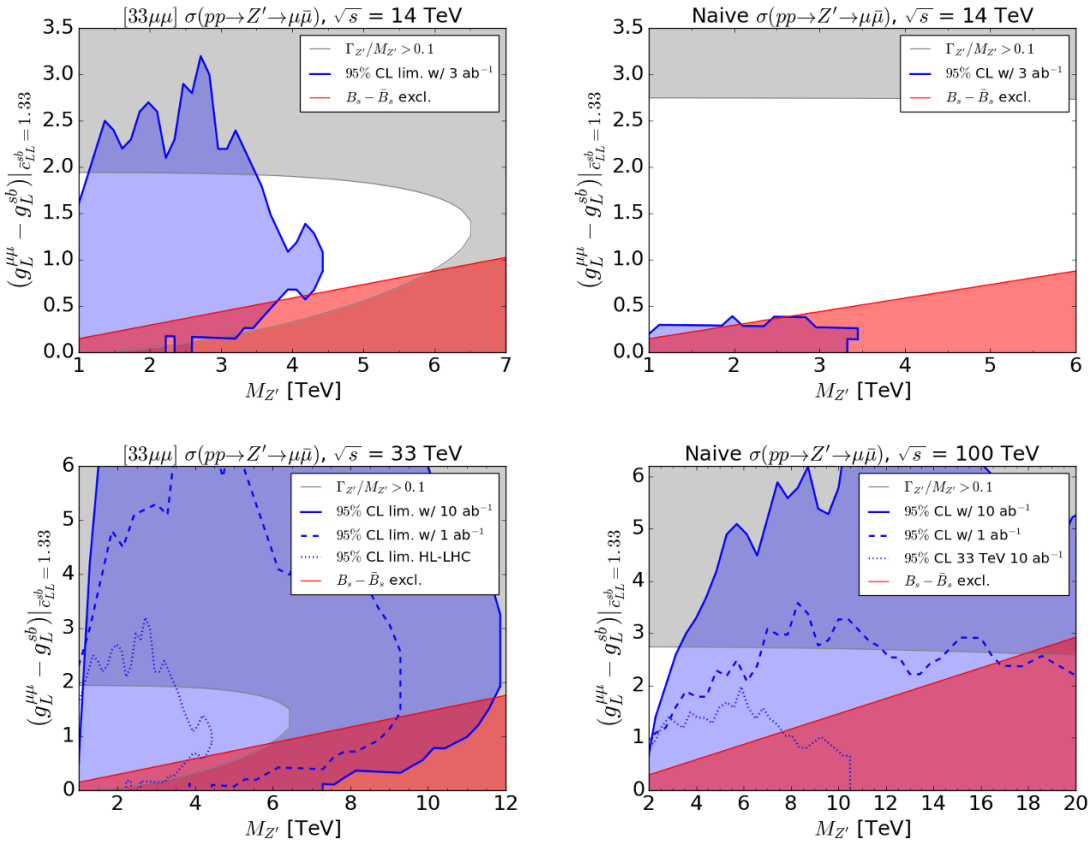

Figure 5. Summary of b-anomaly explaining Z' search sensitivity in the mass-coupling plane for various different future hadron collider options in the naïve model and the $33\mu\mu$ model. The blue shaded region shows the expected sensitivity at the future collider from di-muon resonance searches derived from figure 2. The red region extending to the right hand side of each plot shows the limit coming from $B_s - \bar{B}_s$ mixing measurements. The grey shaded region violates the narrow width approximation.

Between the CM energies of HL-LHC and FCC-hh is the HE-LHC at 33 TeV CM energy, displayed in the bottom row of figure 3 for a Z' mass of 2 TeV on the left and 5 TeV on the right. The sensitivity drops off such that the HE-LHC no longer covers any non-excluded parameter space for $M_{Z'} \gtrsim 7$ TeV.

To illustrate the possible sensitivity to a more realistic model, in figure 4 we show the reach for the $33\mu\mu$ Z' model defined by the Lagrangian of eq. (2.10). There, the couplings to third-generation left-handed quarks induce a coupling to the first two generations of quarks through the CKM matrix. This raises the production cross-section through the additional initial state partonic channels, and also increases the total decay width. In the top left-hand plot we see that a 1.5 TeV Z' is now accessible to the HL-LHC in all of its favoured parameter space, with the top right-hand plot indicating that the new limit of sensitivity of the HL-LHC for this more realistic model is raised to $M_{Z'} \lesssim 4$ TeV. From the bottom two plots, with $M_{Z'} = 5$ (10) TeV on the left (right), we conclude that the 33 TeV HE-LHC at its highest luminosity can cover all the parameter space of interest for

JHEP03(2018)021

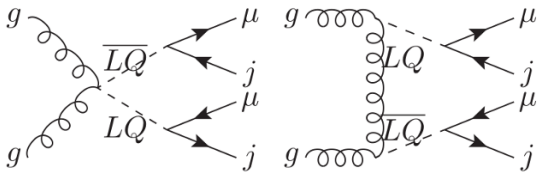

Figure 6. Example Feynman diagrams of LQ production at a hadron collider followed by subsequent decay of each into μj.

all favoured masses. Indeed, we see that for $M_{Z'} \gtrsim 10\,\text{TeV}$ the anomaly-compatible region lies entirely within the grey and red areas and yet is still covered by the blue-shaded area. The FCC-hh with even more energy will therefore also be sensitive to the entire mass range, so we omit its plot.

To summarise the projected reach, we now study the behaviour of the bounds and future collider coverage of Z' models shown in figures 3 and 4 for a continuously varying $M_{Z'}$, shown on the abscissa. We scan along the central green line in those figures, corresponding to the central inferred value of $\bar{c}^{\mu}_{LL} = -1.33$ [28], and plot the value of $g_L^{\mu\mu} - g_L^{sb}$ along this line on the ordinate. We see from the right-hand side plots in figure 5 that the naïve model is not covered much at all by di-muon resonance searches at the LHC, even at high luminosity, but that a 100 TeV 10 ab^{-1} collider can cover all of the viable parameter space where the Z' is narrow (we note that the sensitivity at low masses is underestimated by our limit extrapolation technique, as explained in section 3.1). However, provided the Z' does not dominantly decay to invisible particles, the naïve model is a limiting case that underestimates both the potential sensitivity and the current constraints for a more realistic model. We see in the left-hand plots that in a more complete $33\mu\mu$ model, a 14 TeV 1 ab^{-1} LHC can cover a decent portion of the viable parameter space and a 33 TeV LHC collider is sensitive to all of it.

3.3 LQ sensitivity

There are many dedicated experimental studies of LQs. For some recent examples, CMS have searched for first and second generation LQs in pair production [67–69] and single production [70] at 8 TeV centre of mass energy, while ATLAS set limits on the pair production of third generation LQs using 7 TeV data [71] and first and second generation LQs with 13 TeV [72]. A summary of LQ searches by ATLAS and CMS can be found in ref. [73]. LQs were recently reviewed in refs. [74, 75].

As the basis for our extrapolation, we take the 95 % CL limits from the CMS 8 TeV search for a pair of second generation scalar LQs with 19.6 fb^{-1} of integrated luminosity [67], focusing on the $\mu\mu jj$ channel in particular, as shown in figure 6. The current limits exclude masses up to 1070 GeV, assuming a 100% branching fraction into a charged lepton and quark. We note here that, for scalar LQs, pair production proceeds through the strong interaction and so limits coming from the experimental search may be phrased as only depending on the LQ mass, once the assumption about its branching fraction is made. For vector LQs, the production is more model dependent.

JHEP03(2018)021

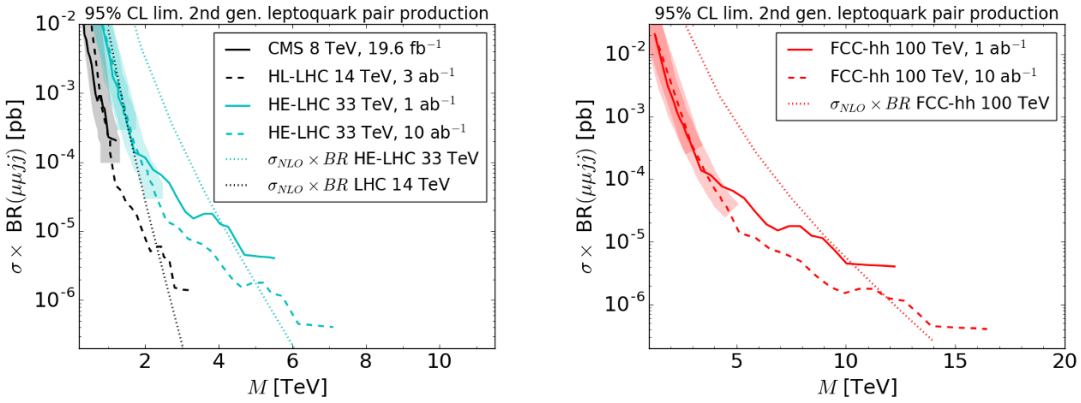

Figure 7. Projected sensitivity of future colliders to di-scalar LQ production (where each decays to a muon and a jet) for the luminosities and centre of mass energies given in the legend. We also show the LQ production cross-section times branching ratio *predicted* for some future collider scenarios by the curves labelled $\sigma_{NLO} \times BR$. Shaded parts of the curve indicate the conservative extrapolation method at low masses that underestimates the actual limit.

We note that the extrapolation procedure detailed in section 3.1 was not strictly designed for this case, which is not production of a simple $s-$channel resonance. However, in practice, di-LQ pair production occurs dominantly at threshold when $\hat{s} = (2M_{LQ})^2$ and so $M = 2M_{LQ}$ is used instead in eq. (3.1) though the resulting exclusion is mostly insensitive to the precise choice of M. Nevertheless, the off-threshold contribution is comparatively larger than for a narrow s-channel resonance and so we expect our extrapolation to be more approximate for extrapolated limits on LQs. After this change to our limit extrapolation procedure, we obtain the weighted sum of parton pair luminosities for the dominant contributions to the background processes, in this case $Z/\gamma^* + \text{jets}$ and $t\bar{t}$, then find the equivalent mass at a future collider that gives the same number of background events. The results for the projected limits are shown in figure 7 for scalar LQs. In the left hand plot, the exclusion curve in solid black is the current CMS 8 TeV exclusion curve, while the dashed black line shows that the LHC reach can be extended for 14 TeV at high luminosity (HL-LHC) with 3 ab^{-1}. The cyan-coloured limits are for a potential high-energy upgrade to the LHC (HE-LHC) that could reach up to 33 TeV centre of mass energy. The solid and dashed lines represent 1 and 10 ab^{-1} of integrated luminosities, respectively. It appears that at low masses, the CMS 8 TeV analysis is more sensitive (when phrased in terms of $\sigma \times BR$) than when the energy is upgraded to 14 TeV at the HL-LHC. This is an artefact of the arbitrariness in the starting point of the extrapolated exclusion curve, as explained in section 3.1, where below this point lower luminosities can set limits at lower masses, though this conservative procedure underestimates the actual limit. The regions below the extrapolated starting point are shaded on top of their respective curves. On the right-hand side of figure 7 we display the limits for a 100 TeV proton-proton future circular collider, the FCC-hh, at 1 (10) ab^{-1} in solid (dashed) red.

The dotted lines superimposed on both plots are theoretical calculations at next-to-leading order for the LQ pair production process, using the code of ref. [76]. Modulo the

JHEP03(2018)021

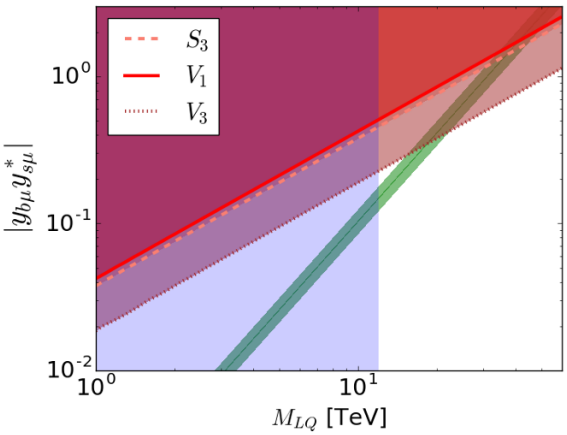

Figure 8. Parameter space of the LQ on a log-log scale for couplings $|y_{b\mu}y^*_{s\mu}|$ vs mass in TeV. The green strip indicates the region compatible with the B-anomalies at 1σ. The different red-shaded regions are excluded by $B_s - \bar{B}_s$ mixing up to the solid red (dotted brown) line for the V_1 (V_3) vector LQ, and up to the dashed pink line for the S_3 scalar LQ, respectively. The region in blue up to $M_{LQ} \sim 12\,\text{TeV}$ is the projected 95% CL limit on scalar LQ pair production for FCC-hh at 100 TeV with 10 ab^{-1}.

$\mathcal{O}(1)$ uncertainties in the excluded cross-section times branching ratio, we see that HL-LHC can exclude LQ masses up to 2 TeV, while HE-LHC can roughly double that to 4 (5) TeV with 1 (10) ab^{-1}. At FCC-hh the limits are improved by an order of magnitude with respect to current searches, reaching exclusions up to 10 and 12 TeV for 1 and 10 ab^{-1}, respectively.

These projected bounds on the LQ mass are to be compared with the upper limit allowed by $B_s - \bar{B}_s$ mixing. The relevant four-fermion operator of the effective Lagrangian for this process can be written as

$$\mathcal{L}_{\bar{b}s\bar{b}s} = c^{bb}_{LL} \left(\bar{b}\gamma_\mu P_L s\right) \left(\bar{s}\gamma^\mu P_L b\right) + \text{h.c.}\,. \tag{3.9}$$

The Wilson coefficient gets a contribution from the coupling combination $|y_{b\mu}y^*_{s\mu}|$ that is given by [25]

$$c^{bb}_{LL} = k \frac{|y_{b\mu}y^*_{s\mu}|^2}{32\pi^2 M^2_{LQ}}\,, \tag{3.10}$$

where $y = y_3, y_1, y'_3$ and $k = 5, 4, 20$ for the S_3, V_1, V_3 LQs, respectively. Using this expression, together with eq. (2.7) and the experimental limit from $B_s - \bar{B}_s$ mixing that constrains $\bar{c}^{bb}_{LL} \lesssim 1/(210\ \text{TeV})^2$ [28], we obtain the parameter space shown in figure 8. The couplings as a function of mass are displayed on a log-log scale, and the green strip represents the parameter space compatible with the B-anomalies at 1σ. The different shades of red are excluded by $B_s - \bar{B}_s$ mixing for the S_3, V_1, V_3 LQs up to the solid red, dotted brown, and dashed pink lines, respectively. We see that the maximal values of the LQ masses allowed by $B_s - \bar{B}_s$ mixing correspond to $M_{LQ} = 37, 41, 18\,\text{TeV}$ for S_3, V_1, V_3, respectively. The blue region shows the 95% CL limits for scalar LQs at a 100 TeV collider with 10 ab^{-1},

JHEP03(2018)021

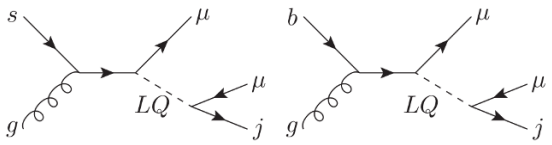

Figure 9. Example Feynman diagrams of single LQ production at a hadron collider followed by its subsequent decay into μj. Note that the LQ production cross-section depends upon its coupling to fermions, in contrast to the pair production cross-section depicted in figure 6.

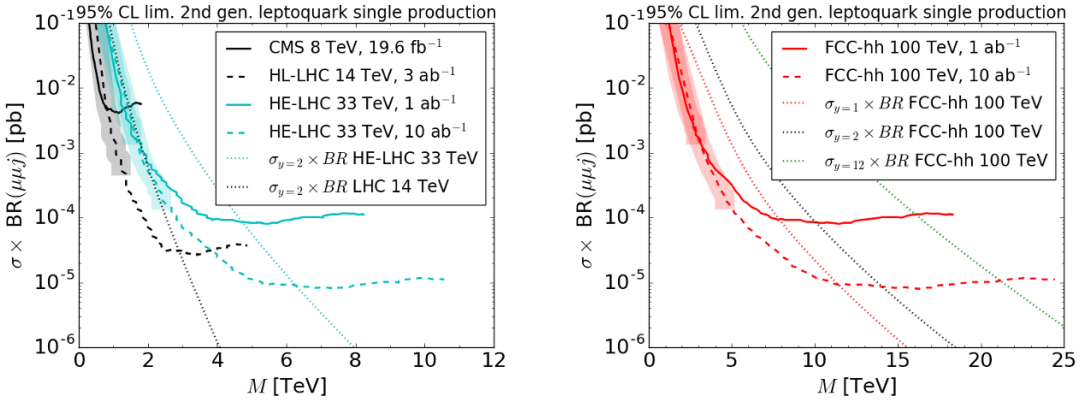

Figure 10. Projected sensitivity of future colliders to single LQ production that decays to a muon and a jet, for the luminosities and centre of mass energies given in the legend. We also show the cross-section times branching ratio for some future collider scenarios by the curves labelled $\sigma_y \times BR$, where y is the scalar LQ coupling to $b\mu$, set equal to the coupling to $s\mu$. Shaded parts of the curve indicate the conservative extrapolation method at low masses that underestimates the actual limit.

such as the FCC-hh. The pair production process for vector LQs is more model-dependent (unlike scalar LQs, whose gluon interactions are fixed by the SU(3)$_c$ gauge couplings) but is typically stronger than the scalar case [77–79].

The direct search sensitivity may also be extended to heavier LQs by considering single LQ production [80], as in figure 9. For large enough couplings the limits may be stronger than those obtained in pair production [70], but the product of the $b\mu$ and $s\mu$ couplings must remain within the stringent bounds from $B_s - \bar{B}_s$ mixing.

We extrapolate the current limits from a direct search by CMS for a single scalar LQ produced at 8 TeV with 19.6 fb^{-1} [70]. CMS places a bound of $M_{LQ} \gtrsim 660$ GeV for a second generation LQ with coupling to $s\mu$ of order unity. For our signal cross-section we also include a $b\mu$ coupling since we take the b quarks to be in the 5-flavour initial parton distribution function NNPDF2.3LO ($\alpha_s(M_Z) = 0.119$) [63]. This re-sums the large logarithms of the initial state b-quark line. We integrate the partonic cross-section with the parton distribution functions using `LHAPDF` [64]. The partonic cross-section at leading order for a scalar LQ ϕ is given by [81]

$$\hat{\sigma}(qg \to \phi l) = \frac{y^2 \alpha_S}{96\hat{s}} \left(1 + 6r - 7r^2 + 4r(r+1)\ln r\right) , \tag{3.11}$$

where $r = M_{LQ}^2/\hat{s}$ and we set $y_{s\mu} = y_{b\mu} = y$ for simplicity. This expression has been

JHEP03(2018)021

cross-checked with figure 8b of ref. [70] and found to agree within partonic uncertainties. The extrapolated limits and production cross-sections for a coupling and branching ratio set to 1 are displayed in figure 10, with the same colour coding as figure 7. The signal cross-sections at 14 and 33 TeV are shown as dotted lines for $y = 1$ in black and cyan respectively, on the left plot. On the right we have the signal cross-section for 100 TeV with $y = 1, 2$, and 12 in red, black, and green dotted lines respectively. We see that for couplings $y = 1$, the limits are comparable to pair production but slightly lower. On the other hand for $y = 2$ the limits at 100 TeV go up to 15 TeV for 10 ab^{-1}, extending to 21 TeV for $y \sim 4\pi$. The reach can be further extended for a model with additional quark couplings. Note however that in a realistic model the product of $y_{b\mu}$ and $y_{s\mu}$ must still be anomaly-compatible within the $B_s - \bar{B}_s$ mixing bounds shown in figure 8, so that these limits only apply when one coupling is taken large with the other small.

4 Conclusion

Some measurements of $B \to K^{(*)} l^+ l^-$ decays disagree with SM predictions: using only theoretically clean quantities, the discrepancy on a Wilson coefficient with respect to the SM value is at around the 4σ level [28]. More specifically, the ratio of decays to muon pairs and electron pairs is predicted to be 1.0 in the SM, but is measured to be lower than this value both for K and K^* in the final state, R_{K^*} in two different bins of transferred 4-momentum (squared). Moreover, the 4σ pull from these clean observables on a Wilson coefficient parameterising new physics is not only statistically significant, but also in the same direction as another independent 4σ pull due to other (less clean) observables. The combined significance in a global fit is then significantly larger than 4σ.

Many authors have constructed bottom-up models containing new particles in order to change the apparent predictions and explain the discrepancies. In particular, it appears that lepton flavour universality should be broken by the new particles, which should have chiral interactions. At tree level, there are only two classes of new particle which explain the discrepancies: flavourful Z's and LQs. We choose these two cases to examine future hadron collider sensitivities: there are other possibilities from particles which affect the decays at the loop level, but because of the loop suppression, these particles should be a factor of roughly 4π lighter than the tree-level cases, and should therefore be easier to detect directly by production in a collider. Studying the tree-level possibilities is then conservative: if one shows that one can discover these, it should be easier to find the lighter particles that are predicted by the loop effects.

We found that for the Z' models, a 100 TeV future collider will essentially cover all of the parameter space that can explain the $B \to K^{(*)} l^+ l^-$ decay data in a resonant di-muon search. Examining more complete models than the naïve Z' model such as the $33\mu\mu$ model, we see that even a 33 TeV run of the LHC may cover all of the relevant viable parameter space. The more complete models contain more model dependence, but have stronger bounds and more coverage than the naïve model. One caveat to our analysis is that we only consider a narrow Z' with width less than a tenth or so of the mass. This will not necessarily be the case, but wide Z's invalidate the procedure we use to extrapolate current bounds from scaling the background detailed in section 3.1, and so require a more

JHEP03(2018)021

detailed simulation of backgrounds and signal at high energies. Nevertheless, a wide Z' is theoretically disfavoured by the large couplings required: they run into Landau poles. The Z' case is summarised in figure 5, where expected sensitivities, bounds and the validity limit of our analysis are plotted for various different future hadron collider assumptions.

Coverage of the relevant LQ models is significant, but somewhat less complete than the Z' models: whilst LQs of varying kinds up to masses of 41 TeV may explain the $B \to K^{(*)}\mu^+\mu^-$ decay data, we show that the expected sensitivity of di-LQ production into a $\mu\mu jj$ final state reaches up to 12 TeV for a scalar LQ. In more model-dependent cases the reach can be higher, as for example in pair production for vector LQs and single production for both vector and scalar LQs, which depend on a choice of couplings. We estimated the sensitivity of single scalar LQ production and found that $\mathcal{O}(1)$ couplings can reach a sensitivity up to LQ masses of around 21 TeV at the strong coupling limit. Whilst our extrapolation of current LHC limits is rather rough (one may expect an uncertainty of a factor of two in the cross-section times branching ratio for the limit due to PDF uncertainties and different detector effects etc.), we estimate that this only results in an uncertainty on the sensitivity of around ± 1 TeV when expressed in terms of the mass of leptoquarks or Z' particles (as evidenced by the steep model prediction curves in figures 7 and 10, for example).

A potential loop-hole in our analysis would occur if one assumed the existence of *multiple* (N) mediators of the c^{μ}_{LL} operator. Under the assumption that each of the N mediators (Z's or LQs) has an equivalent mass and identical couplings, one obtains a contribution to c^{μ}_{LL} that is proportional to either $N|y|^2/M^2$ in the LQ case, or $N g^{sb}_L g^{\mu\mu}_L / M^2_{Z'}$ in the Z' case. For an identical effect on the measured b decays as in the unique mediator case, each of the N mediators could therefore be heavier by a factor $\sqrt{N}$ or more weakly coupled. The LHC mediator production cross-section falls with a power of the mass that is significantly higher than two, resulting in weaker collider sensitivity despite a factor of N from the production of more new mediators.

Of course, there is always the possibility that the current discrepancy with SM predictions is due to a fluke. In this case, our paper still serves a purpose, estimating the reach of future colliders into particular flavourful Z' or LQ models and demonstrating the interplay between indirect and direct searches for new physics. In any case, new empirical data on the $B \to K^{(*)}l^+l^-$ decays are expected from Belle II and LHCb in the next few years. Ref. [82] points out that by 2020, the number of $b\bar{b}$ pairs produced inside the acceptance of LHCb should increase by a factor of 3.7 as compared to those produced before and during 2012. For example, this would result in a discovery of a non-SM effect beyond the 5σ level in R_K, and close to a 5σ level effect in R_{K^*} from LHCb data alone if the central values were not to change from their current values [82].

We have shown that there is significant coverage of all beyond the SM explanations of the current anomalies in proposed future hadron colliders. Thus, if the signal significance of non-SM effects in $B \to K^{(*)}\mu^+\mu^-$ decays increases, so does this particular motivation for higher energy future colliders.[17]

[17] It does not follow that the motivation for going to higher energies then goes away if the anomalies vanish; there are many good reasons (that this margin is too small to contain) for furthering direct experimental exploration of the smallest scales for as long as we have the ability and curiosity to do so.

JHEP03(2018)021

Acknowledgments

We thank other members of the Cambridge SUSY Working Group and Michelangelo Mangano for helpful advice and comments. BCA thanks the Aspen Center for Physics for hospitality offered while part of this work was carried out. TY thanks the Galileo Galilei Institute for hospitality and Nazila Mahmoudi for useful discussions. This work has been partially supported by STFC consolidated grants ST/P000681/1 and ST/L000385/1 and by National Science Foundation grant PHY-1607611. TY is supported by a Junior Research Fellowship from Gonville and Caius College, Cambridge.

JHEP03(2018)021

References

[1] LHCb collaboration, *Test of lepton universality using $B^+ \to K^+\ell^+\ell^-$ decays*, *Phys. Rev. Lett.* **113** (2014) 151601 [arXiv:1406.6482] [INSPIRE].

[2] LHCb collaboration, *Test of lepton universality with $B^0 \to K^{*0}\ell^+\ell^-$ decays*, *JHEP* **08** (2017) 055 [arXiv:1705.05802] [INSPIRE].

[3] G. Hiller and F. Krüger, *More model-independent analysis of $b \to s$ processes*, *Phys. Rev.* **D 69** (2004) 074020 [hep-ph/0310219] [INSPIRE].

[4] BaBar collaboration, J.P. Lees et al., *Evidence for an excess of $\bar{B} \to D^{(*)}\tau^-\bar{\nu}_\tau$ decays*, *Phys. Rev. Lett.* **109** (2012) 101802 [arXiv:1205.5442] [INSPIRE].

[5] BaBar collaboration, J.P. Lees et al., *Measurement of an excess of $\bar{B} \to D^{(*)}\tau^-\bar{\nu}_\tau$ decays and implications for charged Higgs bosons*, *Phys. Rev.* **D 88** (2013) 072012 [arXiv:1303.0571] [INSPIRE].

[6] Belle collaboration, M. Huschle et al., *Measurement of the branching ratio of $\bar{B} \to D^{(*)}\tau^-\bar{\nu}_\tau$ relative to $\bar{B} \to D^{(*)}\ell^-\bar{\nu}_\ell$ decays with hadronic tagging at Belle*, *Phys. Rev.* **D 92** (2015) 072014 [arXiv:1507.03233] [INSPIRE].

[7] Belle collaboration, Y. Sato et al., *Measurement of the branching ratio of $\bar{B}^0 \to D^{*+}\tau^-\bar{\nu}_\tau$ relative to $\bar{B}^0 \to D^{*+}\ell^-\bar{\nu}_\ell$ decays with a semileptonic tagging method*, *Phys. Rev.* **D 94** (2016) 072007 [arXiv:1607.07923] [INSPIRE].

[8] Belle collaboration, S. Hirose et al., *Measurement of the τ lepton polarization and $R(D^*)$ in the decay $\bar{B} \to D^*\tau^-\bar{\nu}_\tau$*, *Phys. Rev. Lett.* **118** (2017) 211801 [arXiv:1612.00529] [INSPIRE].

[9] LHCb collaboration, *Measurement of the ratio of branching fractions $\mathcal{B}(\bar{B}^0 \to D^{*+}\tau^-\bar{\nu}_\tau)/\mathcal{B}(\bar{B}^0 \to D^{*+}\mu^-\bar{\nu}_\mu)$*, *Phys. Rev. Lett.* **115** (2015) 111803 [arXiv:1506.08614] [INSPIRE].

[10] LHCb collaboration, *Measurement of the ratio of the $B^0 \to D^{*-}\tau^+\nu_\tau$ and $B^0 \to D^{*-}\mu^+\nu_\mu$ branching fractions using three-prong τ-lepton decays*, arXiv:1708.08856 [INSPIRE].

[11] S. Descotes-Genon, J. Matias, M. Ramon and J. Virto, *Implications from clean observables for the binned analysis of $B \to K * \mu^+\mu^-$ at large recoil*, *JHEP* **01** (2013) 048 [arXiv:1207.2753] [INSPIRE].

[12] LHCb collaboration, *Differential branching fractions and isospin asymmetries of $B \to K^{(*)}\mu^+\mu^-$ decays*, *JHEP* **06** (2014) 133 [arXiv:1403.8044] [INSPIRE].

[13] LHCb collaboration, *Measurement of form-factor-independent observables in the decay $B^0 \to K^{*0}\mu^+\mu^-$*, *Phys. Rev. Lett.* **111** (2013) 191801 [arXiv:1308.1707] [INSPIRE].

[14] LHCb collaboration, *Angular analysis of the $B^0 \to K^{*0}\mu^+\mu^-$ decay using $3\,fb^{-1}$ of integrated luminosity*, *JHEP* **02** (2016) 104 [arXiv:1512.04442] [INSPIRE].

[15] S. Descotes-Genon, T. Hurth, J. Matias and J. Virto, *Optimizing the basis of $B \to K^*ll$ observables in the full kinematic range*, *JHEP* **05** (2013) 137 [arXiv:1303.5794] [INSPIRE].

[16] S. Descotes-Genon, L. Hofer, J. Matias and J. Virto, *Global analysis of $b \to s\ell\ell$ anomalies*, *JHEP* **06** (2016) 092 [arXiv:1510.04239] [INSPIRE].

[17] BELLE collaboration, A. Abdesselam et al., *Angular analysis of $B^0 \to K^*(892)^0\ell^+\ell^-$*, arXiv:1604.04042 [INSPIRE].

[18] LHCb collaboration, *Angular analysis and differential branching fraction of the decay $B_s^0 \to \phi\mu^+\mu^-$*, *JHEP* **09** (2015) 179 [arXiv:1506.08777] [INSPIRE].

[19] S. Descotes-Genon, J. Matias and J. Virto, *Understanding the $B \to K^*\mu^+\mu^-$ anomaly*, *Phys. Rev.* **D 88** (2013) 074002 [arXiv:1307.5683] [INSPIRE].

[20] W. Altmannshofer and D.M. Straub, *New physics in $B \to K^*\mu\mu$?*, *Eur. Phys. J.* **C 73** (2013) 2646 [arXiv:1308.1501] [INSPIRE].

[21] F. Beaujean, C. Bobeth and D. van Dyk, *Comprehensive Bayesian analysis of rare (semi)leptonic and radiative B decays*, *Eur. Phys. J.* **C 74** (2014) 2897 [*Erratum ibid.* **C 74** (2014) 3179] [arXiv:1310.2478] [INSPIRE].

[22] T. Hurth and F. Mahmoudi, *On the LHCb anomaly in $B \to K^*\ell^+\ell^-$*, *JHEP* **04** (2014) 097 [arXiv:1312.5267] [INSPIRE].

[23] B. Capdevila, A. Crivellin, S. Descotes-Genon, J. Matias and J. Virto, *Patterns of new physics in $b \to s\ell^+\ell^-$ transitions in the light of recent data*, *JHEP* **01** (2018) 093 [arXiv:1704.05340] [INSPIRE].

[24] W. Altmannshofer, P. Stangl and D.M. Straub, *Interpreting hints for lepton flavor universality violation*, *Phys. Rev.* **D 96** (2017) 055008 [arXiv:1704.05435] [INSPIRE].

[25] G. Hiller and I. Nisandzic, *R_K and R_{K^*} beyond the standard model*, *Phys. Rev.* **D 96** (2017) 035003 [arXiv:1704.05444] [INSPIRE].

[26] L.-S. Geng et al., *Towards the discovery of new physics with lepton-universality ratios of $b \to s\ell\ell$ decays*, *Phys. Rev.* **D 96** (2017) 093006 [arXiv:1704.05446] [INSPIRE].

[27] M. Ciuchini et al., *On flavourful easter eggs for new physics hunger and lepton flavour universality violation*, *Eur. Phys. J.* **C 77** (2017) 688 [arXiv:1704.05447] [INSPIRE].

[28] G. D'Amico et al., *Flavour anomalies after the R_{K^*} measurement*, *JHEP* **09** (2017) 010 [arXiv:1704.05438] [INSPIRE].

[29] A. Celis, J. Fuentes-Martin, A. Vicente and J. Virto, *Gauge-invariant implications of the LHCb measurements on lepton-flavor nonuniversality*, *Phys. Rev.* **D 96** (2017) 035026 [arXiv:1704.05672] [INSPIRE].

[30] L. Di Luzio and M. Nardecchia, *What is the scale of new physics behind the B-flavour anomalies?*, *Eur. Phys. J.* **C 77** (2017) 536 [arXiv:1706.01868] [INSPIRE].

JHEP03(2018)021

[31] B.W. Lee, C. Quigg and H.B. Thacker, *Weak interactions at very high-energies: the role of the Higgs boson mass*, *Phys. Rev.* **D 16** (1977) 1519 [INSPIRE].

[32] B.W. Lee, C. Quigg and H.B. Thacker, *The strength of weak interactions at very high-energies and the Higgs boson mass*, *Phys. Rev. Lett.* **38** (1977) 883 [INSPIRE].

[33] J. Ellis, M. Fairbairn and P. Tunney, *Anomaly-free models for flavour anomalies*, arXiv:1705.03447 [INSPIRE].

[34] A. Thamm, R. Torre and A. Wulzer, *Future tests of Higgs compositeness: direct vs indirect*, *JHEP* **07** (2015) 100 [arXiv:1502.01701] [INSPIRE].

[35] G. Salam and A. Weiler, *Collider reach*, http://collider-reach.web.cern.ch/collider-reach/ (2017).

[36] N. Arkani-Hamed, T. Han, M. Mangano and L.-T. Wang, *Physics opportunities of a* 100 *TeV proton–proton collider*, *Phys. Rept.* **652** (2016) 1 [arXiv:1511.06495] [INSPIRE].

[37] J. Baglio, A. Djouadi and J. Quevillon, *Prospects for Higgs physics at energies up to* 100 *TeV*, *Rept. Prog. Phys.* **79** (2016) 116201 [arXiv:1511.07853] [INSPIRE].

[38] T. Golling et al., *Physics at a* 100 *TeV pp collider: beyond the standard model phenomena*, *CERN Yellow Report* (2017) 441 [arXiv:1606.00947] [INSPIRE].

[39] R. Contino et al., *Physics at a* 100 *TeV pp collider: Higgs and EW symmetry breaking studies*, *CERN Yellow Report* (2017) 255 [arXiv:1606.09408] [INSPIRE].

[40] M.L. Mangano et al., *Physics at a* 100 *TeV pp collider: standard model processes*, *CERN Yellow Report* (2017) 1 [arXiv:1607.01831] [INSPIRE].

[41] J. Ellis and T. You, *Sensitivities of prospective future e^+e^- colliders to Decoupled New Physics*, *JHEP* **03** (2016) 089 [arXiv:1510.04561] [INSPIRE].

[42] J. Ellis, P. Roloff, V. Sanz and T. You, *Dimension-6 operator analysis of the CLIC sensitivity to new physics*, *JHEP* **05** (2017) 096 [arXiv:1701.04804] [INSPIRE].

[43] G. Durieux, C. Grojean, J. Gu and K. Wang, *The leptonic future of the Higgs*, *JHEP* **09** (2017) 014 [arXiv:1704.02333] [INSPIRE].

[44] B. Henning, X. Lu and H. Murayama, *What do precision Higgs measurements buy us?*, arXiv:1404.1058 [INSPIRE].

[45] S.-F. Ge, H.-J. He and R.-Q. Xiao, *Probing new physics scales from Higgs and electroweak observables at e^+e^- Higgs factory*, *JHEP* **10** (2016) 007 [arXiv:1603.03385] [INSPIRE].

[46] T. Barklow et al., *Improved formalism for precision Higgs coupling fits*, arXiv:1708.08912 [INSPIRE].

[47] F. Sala and D.M. Straub, *A new light particle in B decays?*, *Phys. Lett.* **B 774** (2017) 205 [arXiv:1704.06188] [INSPIRE].

[48] D. Ghosh, *Explaining the R_K and R_{K^*} anomalies*, *Eur. Phys. J.* **C 77** (2017) 694 [arXiv:1704.06240] [INSPIRE].

[49] K. Fuyuto, W.-S. Hou and M. Kohda, *Z'-induced FCNC decays of top, beauty and strange quarks*, *Phys. Rev.* **D 93** (2016) 054021 [arXiv:1512.09026] [INSPIRE].

[50] A. Datta, J. Liao and D. Marfatia, *A light Z' for the R_K puzzle and nonstandard neutrino interactions*, *Phys. Lett.* **B 768** (2017) 265 [arXiv:1702.01099] [INSPIRE].

JHEP03(2018)021

[51] F. Bishara, U. Haisch and P.F. Monni, *Regarding light resonance interpretations of the B decay anomalies*, *Phys. Rev.* **D 96** (2017) 055002 [arXiv:1705.03465] [INSPIRE].

[52] R. Alonso, B. Grinstein and J. Martin Camalich, SU(2) × U(1) *gauge invariance and the shape of new physics in rare B decays*, *Phys. Rev. Lett.* **113** (2014) 241802 [arXiv:1407.7044] [INSPIRE].

[53] A. Celis, J. Fuentes-Martin, A. Vicente and J. Virto, *DsixTools: the standard model effective field theory toolkit*, *Eur. Phys. J.* **C 77** (2017) 405 [arXiv:1704.04504] [INSPIRE].

[54] D. Ghosh, M. Nardecchia and S.A. Renner, *Hint of lepton flavour non-universality in B meson decays*, *JHEP* **12** (2014) 131 [arXiv:1408.4097] [INSPIRE].

[55] T. Hurth, F. Mahmoudi, D. Martinez Santos and S. Neshatpour, *Lepton nonuniversality in exclusive b→sℓℓ decays*, *Phys. Rev.* **D 96** (2017) 095034 [arXiv:1705.06274] [INSPIRE].

[56] B. Allanach, F.S. Queiroz, A. Strumia and S. Sun, *Z′ models for the LHCb and g − 2 muon anomalies*, *Phys. Rev.* **D 93** (2016) 055045 [arXiv:1511.07447] [INSPIRE].

[57] R.S. Chivukula, J. Isaacson, K.A. Mohan, D. Sengupta and E.H. Simmons, R_K *anomalies and simplified limits on Z′ models at the LHC*, *Phys. Rev.* **D 96** (2017) 075012 [arXiv:1706.06575] [INSPIRE].

[58] D. Buttazzo, A. Greljo, G. Isidori and D. Marzocca, *B-physics anomalies: a guide to combined explanations*, *JHEP* **11** (2017) 044 [arXiv:1706.07808] [INSPIRE].

[59] I. Doršner, S. Fajfer, D.A. Faroughy and N. Košnik, *The role of the S_3 GUT leptoquark in flavor universality and collider searches*, arXiv:1706.07779 [INSPIRE].

[60] A. Greljo and D. Marzocca, *High-p_T dilepton tails and flavor physics*, *Eur. Phys. J.* **C 77** (2017) 548 [arXiv:1704.09015] [INSPIRE].

[61] ATLAS collaboration, *Search for high-mass new phenomena in the dilepton final state using proton-proton collisions at $\sqrt{s} = 13$ TeV with the ATLAS detector*, *Phys. Lett.* **B 761** (2016) 372 [arXiv:1607.03669] [INSPIRE].

[62] J. Alwall et al., *The automated computation of tree-level and next-to-leading order differential cross sections and their matching to parton shower simulations*, *JHEP* **07** (2014) 079 [arXiv:1405.0301] [INSPIRE].

[63] R.D. Ball et al., *Parton distributions with LHC data*, *Nucl. Phys.* **B 867** (2013) 244 [arXiv:1207.1303] [INSPIRE].

[64] A. Buckley et al., *LHAPDF6: parton density access in the LHC precision era*, *Eur. Phys. J.* **C 75** (2015) 132 [arXiv:1412.7420] [INSPIRE].

[65] M. Lim, F. Maltoni, G. Ridolfi and M. Ubiali, *Anatomy of double heavy-quark initiated processes*, *JHEP* **09** (2016) 132 [arXiv:1605.09411] [INSPIRE].

[66] M. Dalchenko et al., *Bottom-quark fusion processes at the LHC for probing Z′ models and B-meson decay anomalies*, arXiv:1707.07016 [INSPIRE].

[67] CMS collaboration, *Search for pair-production of first generation scalar leptoquarks in pp collisions at $\sqrt{s} = 8$ TeV*, CMS-PAS-EXO-12-041 (2012).

[68] CMS collaboration, *Search for Pair-production of Second generation Leptoquarks in 8 TeV proton-proton collisions*, CMS-PAS-EXO-12-042 (2012).

JHEP03(2018)021

[69] CMS collaboration, *Search for pair production of first and second generation leptoquarks in proton-proton collisions at* $\sqrt{s} = 8$ *TeV*, *Phys. Rev.* **D 93** (2016) 032004 [arXiv:1509.03744] [INSPIRE].

[70] CMS collaboration, *Search for single production of scalar leptoquarks in proton-proton collisions at* $\sqrt{s} = 8$ *TeV*, *Phys. Rev.* **D 93** (2016) 032005 [arXiv:1509.03750] [INSPIRE].

[71] ATLAS collaboration, *Search for third generation scalar leptoquarks in pp collisions at* $\sqrt{s} = 7$ *TeV with the ATLAS detector*, *JHEP* **06** (2013) 033 [arXiv:1303.0526] [INSPIRE].

[72] ATLAS collaboration, *Search for scalar leptoquarks in pp collisions at* $\sqrt{s} = 13$ *TeV with the ATLAS experiment*, *New J. Phys.* **18** (2016) 093016 [arXiv:1605.06035] [INSPIRE].

[73] ATLAS and CMS collaborations, *Search for leptoquark-like signatures with the ATLAS and CMS detectors*, *Nucl. Part. Phys. Proc.* **273-275** (2016) 638 [INSPIRE].

[74] I. Doršner et al., *Physics of leptoquarks in precision experiments and at particle colliders*, *Phys. Rept.* **641** (2016) 1 [arXiv:1603.04993] [INSPIRE].

[75] B. Diaz, M. Schmaltz and Y.-M. Zhong, *The leptoquark Hunter's guide: Pair production*, *JHEP* **10** (2017) 097 [arXiv:1706.05033] [INSPIRE].

[76] M. Krämer, T. Plehn, M. Spira and P.M. Zerwas, *Pair production of scalar leptoquarks at the CERN LHC*, *Phys. Rev.* **D 71** (2005) 057503 [hep-ph/0411038] [INSPIRE].

[77] J.L. Hewett, T.G. Rizzo, S. Pakvasa, H.E. Haber and A. Pomarol, *Vector leptoquark production at hadron colliders*, talk given at the *Workshop on Physics at Current Accelerators and the Supercollider*, June 2–5, Argonne, U.S.A. (1993), hep-ph/9310361 [INSPIRE].

[78] T.G. Rizzo, *Searches for scalar and vector leptoquarks at future hadron colliders*, *eConf* **C 960625** (1996) NEW151 [hep-ph/9609267] [INSPIRE].

[79] J.L. Hewett and T.G. Rizzo, *Much ado about leptoquarks: a comprehensive analysis*, *Phys. Rev.* **D 56** (1997) 5709 [hep-ph/9703337] [INSPIRE].

[80] A. Belyaev, C. Leroy, R. Mehdiyev and A. Pukhov, *Leptoquark single and pair production at LHC with CalcHEP/CompHEP in the complete model*, *JHEP* **09** (2005) 005 [hep-ph/0502067] [INSPIRE].

[81] J.L. Hewett and S. Pakvasa, *Leptoquark production in hadron colliders*, *Phys. Rev.* **D 37** (1988) 3165 [INSPIRE].

[82] J. Albrecht et al., *Future prospects for exploring present day anomalies in flavour physics measurements with Belle II and LHCb*, arXiv:1709.10308 [INSPIRE].

JHEP03(2018)021